



J. Serb. Chem. Soc. 88 (6) 653–667 (2023)
JSCS–5653

Use of Jamun seed (*Syzyum cumini*) biochar for the removal of Fuchsin dye from aqueous solution

DIVYA KOSALE, CHANDRAKANT THAKUR and VINOD KUMAR SINGH*

*Department of Chemical Engineering, National Institute of Technology Raipur,
Raipur 492010, Chhattisgarh, India*

(Received 30 August, revised 25 October 2022, accepted 9 April 2023)

Abstract: The textile, leather, paint and other industries discharge lots of dyes in their effluent which can cause major impact to environment and human life. Therefore, it becomes necessary to eliminate the dye from the effluent before its discharge and reuse. Several procedures for the removal and inactivation of dyes have been proposed over past, but the adsorption has gained popularity due to its efficiency and operational ease. Use of the biochars as an adsorbent is gaining attention due to their low cost, availability and high adsorption capability. The current study focuses on the removal of basic Fuchsin (BF) dye by adsorption using Jamun (*Syzyum cumini*) seed powder biochar as an adsorbent. The biochar was characterized through various analyses such as: XRD, EDS, FTIR, TGA and SEM. Adsorption was studied by varying the parameters such as pH, contact duration, temperature, adsorbent dose, and temperature. Further, the isotherm, kinetic and thermodynamic studies were also performed to understand the adsorption mechanism. The maximum adsorption capacity for BF dye was found with Jamun seed biochar produced at 500 °C. The study reveals that the biochar manufactured from Jamun seed powder has a significant potential for the elimination of BF dye from wastewater.

Keywords: adsorption; pyrolysis; TGA; isotherm; kinetics; thermodynamics.

INTRODUCTION

The cosmetics, textiles, paper, pharmaceuticals and leather industries consume enormous quantities of dyes and chemicals during the processing of raw materials and the making of different products. Accordingly, they generate large volumes of dyes-containing liquid effluents which need to be treated for the removal of dyes prior to their disposal, as the untreated waste water may impart toxicity to aquatic life and damage the quality of receiving water bodies and environment.¹ There are different treatment techniques which have been used for

* Corresponding author. E-mail: vksingh.che@nitrr.ac.in
<https://doi.org/10.2298/JSC220830021K>

the reduction of dye such as advanced oxidation, ozonation, adsorption, coagulation/flocculation, aerobic and anaerobic degradation, membrane filtration, *etc.*²⁻⁵ Each technique is having its own advantages and drawbacks but the adsorption has got a lot of attention because of its operational ease, low cost, flexibility, design simplicity, efficiency and profitability.⁶

India's textile sector consumes almost 80% of the overall production of 130,000 tons of dyestuff,⁷ which include non-biodegradable dye in the concentrations ranging from 1 to 2500 mg L⁻¹.⁸ There are about 100,000 commercially available dyes⁹ and basic Fuchsin (BF) dye is one of widely used dye in the textile sector. Due to its toxicity the BF dye can cause several health issues such as skin infection, nausea irritation, vomiting and diarrhoea, damages organs like spleen, thyroid and liver. Also, its inhalation can result in respiratory irritation.¹⁰ BF dye is also known by the name basic violet 14, chemically known as triaminotriphenylmethane (C₂₀H₂₀ClN₃). It is the combination of three dyes namely, pararosaniline, rosaniline and Magenta II.¹¹ BF dye is commonly used for colouring of textile and leather products.¹²

There are many researchers who have worked on BF dye removal through adsorption process using different types of adsorbents such as bottom ash, deoiled soya, graphite oxide, polymer nanocomposite, kola nut pod carbon, eggshell and euryale ferox salisbury seed shell, *etc.*^{10,13-17} Among these adsorbents biomass has gained major attention of the researchers due to its easy availability and low cost. The biochar derived from the biomass of *Syzygium cumini* has been selected as an adsorbent for this study. *Syzygium cumini* is locally known as Jamun (black plum). India produces around 15.4 % of the total world production of Jamun (approximately 13.5 million tons) and its rank is second. Maharashtra is the main producer of Jamun followed by Uttar Pradesh, Tamil Nadu, Gujarat and Assam.¹⁸ Large quantity of Jamun seeds are discarded into open area as waste. The aim of this study is to use these seeds to prepare biochar for the degradation of BF dye from the aqueous solution. No previous studies were found using Jamun seed powder biochar (JSPB) as an adsorbent for the BF dye removal. That is why JSPB was selected as an adsorbent for the reduction of BF dye through batch adsorption process. The Jamun seed powder (JSP) and JSPB were characterized using various techniques like scanning electron microscopy (SEM), X-ray diffraction (XRD), Fourier transform infrared spectroscopy (FTIR), energy dispersive X-ray spectroscopy (EDS) and thermal gravimetric analysis (TGA); the batch adsorption experiments were conducted by varying different parameters. The linear and non-linear form of Langmuir, Freundlich and Temkin isotherm models were applied to understand the mechanism of adsorption process. Kinetic study for this process was done using pseudo 1st and pseudo 2nd order kinetic models. The behaviour of the adsorption process was determined by a thermodynamic study.

EXPERIMENTAL

Materials

BF dye was purchased from Titan Biotech Ltd., Bhiwadi, Rajasthan, India. Its chemical structure is given in Fig. 1.¹⁹ Dried Jamun fruits were purchased from the local market. NaOH and HCl were purchased from Sigma–Aldrich, India, and used for pH adjustment of the dye solution. Distilled water was used for the preparation of all dye solutions.

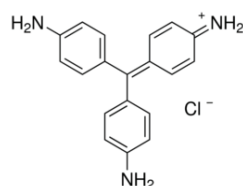


Fig. 1. Structure of basic Fuchsin dye.

Preparation of adsorbent

Dried Jamun fruits were soaked in water for 48 hrs followed by its peeling for seed separation. The seeds were dried in the hot air oven at the temperature 383 K for 36 h and broken down into small pieces using mortar pestle. The pieces of the seeds were ground using mixer grinder followed by screening to get the powder having an average particle size of 49 μm . The screening operation was completed by using 300 and 350 mesh British standard sieve (BSS). JSP was pyrolyzed in a pit type furnace reactor (S. D. Scientific, Kolkata make) at 773 K for 60 min. The resultant Jamun seed powder biochar (JSPB) was taken out from the reactor and kept in air tight container at room temperature for further experiments.

Preparation of adsorbate

A dye solution of 1000 mg L^{-1} was prepared by dissolving the 1mg of BF dye in the 1000 mL of distilled water. The stock solution was then diluted to the desired concentrations of 100, 75, 50, 25, 12.5, 6.25 and 3.125 mg L^{-1} . pH was tuned to the desired value using 0.1 M NaOH and 0.1 M HCl solution. λ_{max} of 548 nm was the maximum absorbance wavelength and hence used as the basis for all the experiments to evaluate the BF dye concentration.

Characterizations of JSP and JSPB

JSP, JSPB before adsorption and JSPB after adsorption were characterised using different techniques. SEM (Zeiss EVO 18) and field emission scanning electron microscopy (FESEM, Carl Zeiss Uhr FESEM model Gemini SEM 500 KMAT) were used for the morphological study and the presence of different elements was found using EDS (INCA 250 EDS). XRD technique was used to find out the structure (crystalline or amorphous) of the samples. FTIR (Alfa, Bruker, Germany) spectroscopy was performed with IR-Affinity-1, Shimadzu, to find the functional groups in the sample by recording the spectra between the frequency ranges of 400–4000 cm^{-1} . The thermal behaviour of the JSP sample was studied by TGA (Setaram Labsys EVO) in the temperature range of 30–850 $^{\circ}\text{C}$.

Batch adsorption experiment

The adsorption experiments were conducted by varying different parameters to examine the adsorption characteristics of JSPB for the removal of BF dye from synthetic solution. For batch process, 100 mL of the dye solution (3–100 mg L^{-1}) with a 0.1–1.0 g of JSPB was taken in the conical flask and shaken in the orbital shaker at 95 ± 5 rpm for time 15–120 min, at pH 2.03–10.02, and temperature 298–338 K. After shaking, the suspensions were filtered and the

BF dye concentration in the supernatant solution was measured with the help of UV–Vis spectrophotometer (LabIndia 3092). The absorbance values at specified wavelength (λ_{\max} of 548 nm) of the samples were recorded, and the equivalent dye concentration value was obtained from the calibration graph. The adsorption capacity, q_e , and the percentage of dye removal, R , were calculated using following equations, respectively:²⁰

$$q_e = \frac{(c_i - c_f)V}{m} \quad (1)$$

$$R = 100 \frac{c_i - c_f}{c_i} \quad (2)$$

where V = volume of BF dye solution (mL), c_i = initial BF dye concentration (mg L^{-1}), m = mass of JSBP (g) and c_f = final concentration of BF dye at equilibrium (mg L^{-1}).

RESULTS AND DISCUSSION

Characterizations of JSP and JSPB

The surface characteristics and morphological features of JSP before adsorption and JSPB after adsorption were determined by the SEM analysis and the images are shown in Fig. 2. The image of raw sample of JSP shows uneven structures with less porous surface whereas the image of JSPB shows porous structures developed during the pyrolysis. After the adsorption of BF dye, the surface of JSPB became comparatively smooth as the pores get filled up with molecules of dye. The elemental composition (% weight basis) of JSP and JSPB before adsorption was determined by the EDS analysis and the results are given in Table I. The JSP surface contains various elements such as carbon, oxygen, nitrogen, silicon, sulphur and potassium. After the pyrolysis, the weight percentage of some of these elements (carbon, silicon and potassium) in the JSPB surface increased and that of oxygen decreased. Also, the presence of new elements like iron and manganese has been observed. The increased percentage of the elements and the addition of new elements may result in the improvement of the adsorption capacity of JSPB.

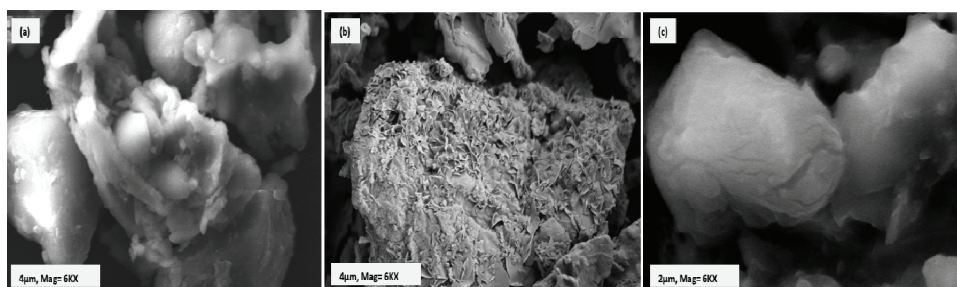


Fig. 2. SEM image of: a) raw JSP 2, b) JSPB before adsorption and c) JSPB after adsorption.

The XRD spectra for raw JSP, JSPB before adsorption and JSPB after adsorption are presented in Fig. 3a. The graph of raw JSP shows non-crystalline

peak with low intensity at an angle of 26.70° , whereas the graph for JSPB has more peaks with slightly increased intensities at the angles 26.70 , 31.51 , 50.08 and 59.98° . It clearly indicates the semi-crystalline nature of JSPB surface which will favour the adsorption process. After the adsorption, the peak at an angle of 26.70° is slightly decreased and some peaks have disappeared, which confirms the successful adsorption of BF dye on JSPB surface.²¹

TABLE I. EDS analysis of JSP and JSPB

No.	Raw JSP		JSPB	
	Element	Weight, %	Element	Weight, %
1	C	18.08	C	40.20
2	O	71.61	O	47.98
3	N	6.23	Mg	1.76
4	Si	1.54	Si	4.51
5	S	0.07	K	3.76
6	K	1.79	Fe	1.78

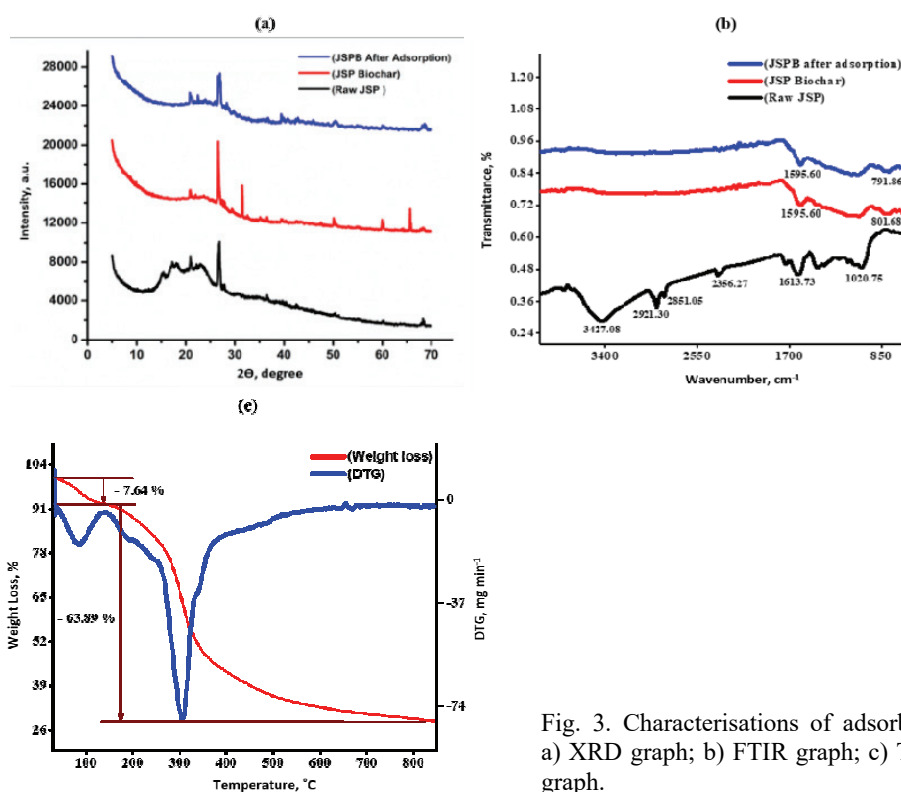


Fig. 3. Characterisations of adsorbent; a) XRD graph; b) FTIR graph; c) TGA graph.

FTIR spectra of raw JSP, JSPB before adsorption and JSPB after adsorption between $400\text{--}4000\text{ cm}^{-1}$ are shown in Fig. 3b. The raw JSP shows a broad-band

around 3427 cm^{-1} indicating O–H stretching (alcohol group). Also, this peak shows the presence of cellulosic components. The band at 2921.30 cm^{-1} confirms the presence of alkyl groups which is the indication of asymmetric C–H band alkyl groups (methyl and methylene group). The band around 2851.05 cm^{-1} , is attributed to H–C=O; C–H stretching vibrations of alkanes groups, whereas the band 2356.27 cm^{-1} is assigned to the amino related component (–N–H component).²² The band 1613.73 cm^{-1} (C=C ring stretching) corresponds to aromatic compounds. Aliphatic ether C–O and alcohol (C–O stretching) components were confirmed by the peak of 1020.75 cm^{-1} . After pyrolyzing the sample all strong peaks like hexagonal, alkyl and alkanes groups disappeared, whereas aromatic groups are still visible. The shallow peaks were observed in both the samples of JSPB before adsorption and JSPB after adsorption, at the band 1595.60 and $801.68\text{--}791.96\text{ cm}^{-1}$, which can be assigned to aromatic group (C=C ring stretching) and 2 adjacent H deformation, respectively.²³ These functional groups may assist in the adsorption of dye molecules on the surface of JSPB.

TGA analysis of raw JSP was performed in the temperature range $30\text{--}850\text{ }^{\circ}\text{C}$. Two weight-loss peaks were found which are shown in Fig. 3c. The first peak was observed with a weight loss of 7.64 % below $100\text{ }^{\circ}\text{C}$, which indicates the dissociation of water molecules from the JSP biomass. The reduction of hemicellulose, cellulose and lignin from the sample was detected by the second peak in the temperature range of $200\text{--}300\text{ }^{\circ}\text{C}$ with a maximum weight loss of 63.89 %. After $300\text{--}400\text{ }^{\circ}\text{C}$, the sample began to deform, and at higher temperatures the peak seemed almost flat and it was decomposed before its reached $850\text{ }^{\circ}\text{C}$. This is the sign of complete pyrolyzation of JSP biomass. Therefore, $500\text{ }^{\circ}\text{C}$ is considered for pyrolysis process.²⁴

Batch adsorption study with effect of various parameters

Effect of concentration. The dye removal in the adsorption study is strongly influenced by the initial dye concentration. The initial concentrations of BF dye were varied from $3\text{--}100\text{ mg L}^{-1}$ at pH 8.01, dosage 0.6 g, contact time 75 min, and the temperature 318 K. The effect of initial dye concentration on the removal has been shown in Fig 4a. It is clear from the plot that the sorption of dye is increasing from 54 to 97% (adsorption capacity increasing from $0.1\text{--}8\text{ mg g}^{-1}$) with the solution concentration. The reason for this may be due to the availability of more dye molecules for the limited binding sites on the adsorbent surface accounts for the rise in BF adsorption.^{25,26} On the other hand, higher initial dye concentration causes an increase in surface use of the adsorbent because of the enhanced contact between adsorbate and adsorbent. The same trend was also observed by Bessashia *et al.* for BF dye.²⁷ The maximum removal efficiency was found to be 97 % with the concentration of 100 mg L^{-1} .

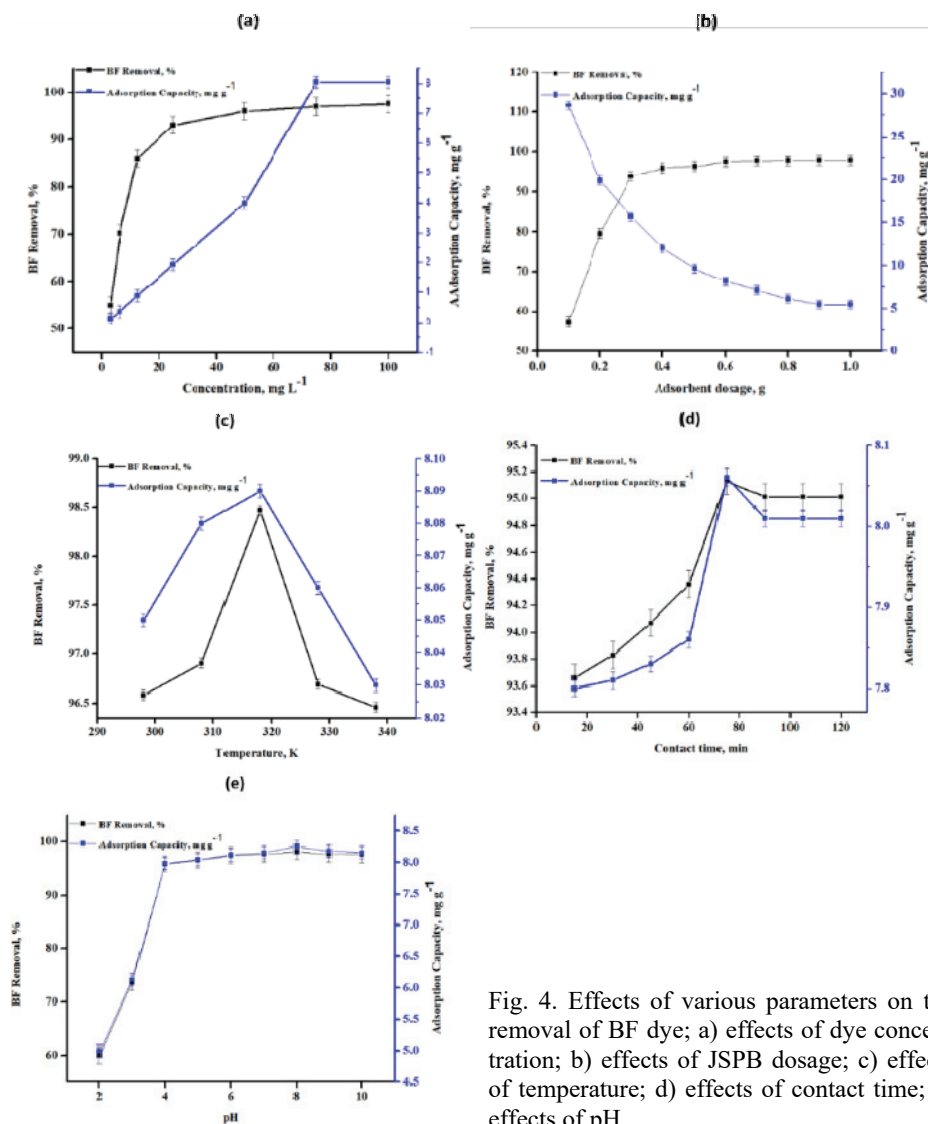


Fig. 4. Effects of various parameters on the removal of BF dye; a) effects of dye concentration; b) effects of JSPB dosage; c) effects of temperature; d) effects of contact time; e) effects of pH.

Effect of adsorbent dosage. The JSPB dosages were varied from 0.1 to 1 g in the amount of liquid 50 ml for each sample at the optimum parameters of contact time 75 min, temperature 318 K and pH 8.01 (Fig. 4b). With the increasing adsorbent dose (0.1 to 1.0 g), the removal percentage is also increasing (55.54–95.56 %) initially (up to 0.6 g), but no significant change occurs later on. This is due to the fact that the dye molecules have occupied the available surface. On the other hand, as the adsorbent dose increases from 0.1 to 1.0 g, the adsorption capacity decreases dramatically from 28.67 to 5.18 mg g⁻¹. As the JSPB dose inc-

reases, the adsorbent particles continually aggregate or agglomerate. Thus, the surface area per unit weight of the adsorbent is reduced, and the diffusion route length increases. This results in a continuous loss of adsorption capacity. For further experiments, 0.6 g of the adsorbent dose was finalised because of its benefits and drawbacks in terms of removal efficiency and adsorption capacity.²⁸

Effect of pH. The pH study was performed at the optimum parameters as adsorbent dosage 0.6 g, temperature 318 K, concentration 100 mg L⁻¹ and time 75 min. The percentage removal was observed to be increasing with pH from 2.03–10.02 (increasing adsorption capacity 4–8 mg g⁻¹) as shown in Fig. 4e. This trend can be understood from the fact that at lower pH, the concentration of H⁺ in a solution remains higher, which will lead to the protonation of active sites of the adsorbent. Since the BF dye is also positively charged, there will be a repulsive force between the adsorbent and adsorbate resulting in less adsorption. At higher pH, H⁺ concentration is lower and hence higher percentage removal can be obtained.²⁹

Effect of contact time. Completion of the process within a short time is extremely important for industrial applications, in terms of cost-effectiveness and efficiency. The influence of contact time (15–120 min) on the uptake dye solution is shown in Fig. 4d. While performing this experiment other parameters were kept constant (pH 8.01, concentration 100 mg L⁻¹, temperature 318 K and dosage 0.6 g). These results show that the adsorption of dye increases with contact time (removal of 93–95 %, adsorption capacity 6–8 mg g⁻¹) and it remains constant after the equilibrium time of 75 min. This may be because of the availability of more active sites initially on JSBP for the dyes and also due to the rate at which the BF dye solution is transferred from the exterior to the interior sites of the JSBP particles, which controls the uptake rate as the surface adsorption sites become exhausted.³⁰

Effect of temperature. The effect of temperature is another significant physicochemical process parameter because the temperature changes the adsorption capacity of the adsorbent. The temperature effect on BF dye removal was studied at the optimum conditions of pH 8.01, contact time 75 min, dosage 0.6 g and concentration 100 mg L⁻¹, Fig. 4c. As the percentage removal of dye increased from 96.58–98.47 % with the increase in temperature from 298 K–318 K, the process shows the endothermic behaviour. With the further temperature rise the removal is decreasing in the temperature range 318 K–338 K, which indicates the exothermic nature of the process. Thus, the temperature study shows the change in nature of the process from endothermic to exothermic. This may be due to the decrease of the quantity of the dye molecules and the active sites on the adsorbent with increasing temperature. Also, the swelling of internal surface of JSBP and the increasing mobility of dye ions at higher temperatures leads to poor adsorption capacity of the adsorbent. This pattern was also observed by Abdus *et al.*^{31,32}

Isotherms, kinetics and thermodynamic study

Isotherm study. The relationship between adsorption capacity and equilibrium concentration is well understood by the adsorption isotherm models. The graph plotted between the solid phase and liquid phase concentration of the JSPB illustrates the equilibrium adsorption isotherms. The linear and nonlinear form of Langmuir, Freundlich and Temkin isotherms were used to describe the experimental data of adsorption for this study. For the analysis of adsorption isotherms, the experiments were conducted at pH 8.01 by adding a 0.6 g of JSPB with 50 ml of BF dye solution and by varying concentrations from 12.5 to 100 mg L⁻¹. JSPB was separated from the solution after 75 min and the concentration of BF dye was estimated using UV spectrophotometer. The experimental and calculated data are summarized in Table II for all the three isotherms.^{11,33}

TABLE II. Freundlich, Langmuir and Temkin constants of linear and nonlinear isotherms for adsorption of dye

Isotherm	Constant	Temperature , K		
		303	308	328
Langmuir	$q_m / \text{mg g}^{-1}$	5.45	50.25	14.89
	$K_L / \text{L mg}^{-1}$	0.67	0.05	0.23
	R^2 (Linear)	0.93	0.94	0.92
	R^2 (Non-linear)	0.88	0.85	0.85
	R_L	0.02	0.15	0.05
Freundlich	n	0.09	0.10	0.11
	$K_f / \text{L g}^{-1}$	0.002	0.006	0.021
	R^2 (Linear)	0.88	0.88	0.87
	R^2 (Non-linear)	0.99	0.91	0.84
	$A_T / \text{L mg}^{-1}$	0.57	0.58	0.36
Temkin	$B_T / \text{J mol}^{-1}$	37.7	31.8	30.2
	R^2 (Linear)	0.99	0.99	0.99
	R^2 (Non-linear)	0.99	0.99	0.99

The Langmuir isotherm is applicable for homogeneous adsorption process, in which there is no contact between the adsorbed molecules due to the monolayer adsorption. Nonlinear and linear form of Langmuir equations are given as:

$$q_e = \frac{q_m K_L c_e}{1 + K_L c_e} \quad (3)$$

$$\frac{1}{q_e} = \frac{1}{K_L q_m} \frac{1}{c_e} + \frac{1}{q_m} \quad (4)$$

where q_m is the maximum adsorption capacity (mg g⁻¹), q_e denotes equilibrium adsorption capacity (mg g⁻¹) and c_e is concentration of BF dye solution at equilibrium (mg L⁻¹). The plots of linear and shows low value of the R^2 , which

indicates that the given adsorption data is not suitable for Langmuir isotherm. The separation factor (R_L) of this isotherm is represented as:

$$R_L = \frac{1}{1 + K_L c_i} \quad (4)$$

where c_i and K_L are the initial concentration and Langmuir constant, respectively. The positive value of R_L ($0 < R_L < 1$), shows the feasibility of process.

Freundlich isotherm is valid for multilayer adsorption and the heterogeneous nature of the process. The non-linear and linear form of Freundlich equations are:

$$q_e = K_f c_e^{\frac{1}{n}} \quad (6)$$

$$\log q_e = \log K_f + \frac{1}{n} \log c_e \quad (7)$$

where the adsorption capacity is measured by intercept $\log K_f$ (Freundlich constant) and the adsorption intensity is represented by the slope $1/n$. The linear and non-linear plots were used to calculate the values of K_f and n . The value of n is 0.11 which is less than 1, and therefore indicates poor adsorption and suggests that the adsorption data does not fit to this isotherm.

The Temkin isotherm model assumes that the heat of adsorption of all molecules in the layer decreases linearly with coverage due to the adsorbate–adsorbent repulsions. It also implies that adsorption occurs as a result of a homogenous binding energy distribution.¹¹ The Temkin non-linear and linear equation can be given as:

$$q_e = \frac{RT}{B_T} \ln(A_T c_e) \quad (8)$$

$$q_e = B_T \ln A_T + B_T \ln c_e \quad (9)$$

$$B_T = \frac{RT}{b} \quad (10)$$

where R = universal gas constant ($8.314 \text{ J mol}^{-1} \text{ K}^{-1}$), T (K) = absolute temperature, A_T (L mg^{-1}) = equilibrium binding constant, B_T = heat of adsorption, B = Temkin constant (J mol^{-1}).

The higher values of R^2 for both the nonlinear and linear form of this model suggest that the Temkin isotherm is the most favourable for the adsorption data. Positive value of B_T is a sign of the exothermic nature of the process.

Kinetic study. Efficiency, mechanism and potential rate controlling step (including mass transfer and chemical reaction) of the adsorption process were determined by the kinetic study. The necessary time for the adsorption kinetics was determined by conducting the experiment in the orbital shaker for a period of 15–75 min (concentrations 25–100 mg L^{-1} at pH 8.01, dosage 0.6 g, and the tempe-

perature 318 K). The samples were taken out from the shaker at an interval of 15 min. Data obtained from the kinetic experiments were evaluated for both linear and nonlinear form of pseudo 1st and pseudo 2nd order and are summarised in Table III.^{34,35}

Pseudo-first-order kinetic model is used to describe the kinetics of many adsorption systems. The nonlinear and linear equations for this model are expressed as follows:

$$q_t = q_e \left(1 - e^{-K_1 t}\right) \quad (11)$$

$$\ln(q_e - q_t) = \ln(K_1 q_e) - K_1 t \quad (12)$$

where K_1 = rate constant of pseudo 1st (L min⁻¹), q_t = adsorption capacity at time t (mg g⁻¹).

TABLE III. Linear and non-linear kinetic parameters for BF dye adsorption

$c / \text{mg L}^{-1}$	$q_{e,\text{exp}}$ mg g^{-1}	Pseudo 1 st order				Pseudo 2 nd order			
		$q_{e,\text{cal}}$ mg g^{-1}	K_1	R^2 (Linear)	R^2 (Nonlinear)	$q_{e,\text{cal}}$ mg g^{-1}	K_1	R^2 (Linear)	R^2 (Nonlinear)
12.5	0.899	0.463	-0.0002	0.86	0.80	0.913	0.665	0.99	0.97
25	1.956	0.230	-0.0003	0.85	0.94	1.945	4.735	1	0.94
50	4.019	0.446	-0.0004	0.83	0.81	3.980	1.062	1	0.92
100	8.029	0.517	-0.0001	0.49	0.88	8.019	0.182	0.99	0.99

The values of K_1 and q_e were calculated from the slopes and intercepts of the plot between $\ln(q_e - q_t)$ and time. On the basis of lower correlation coefficients, it is confirmed that the adsorption of BF dye on JSPB does not involve pseudo first order kinetics.

Pseudo 2nd order kinetic model stated that the rate of occupation of adsorption sites is proportional to the square of number of unoccupied sites. The non-linear equation of this model is given below:

$$\frac{dq_t}{dt} = K_2 (q_e - q_t)^2 \quad (13)$$

$$\frac{1}{q_t} = \frac{1}{K_2 q_e^2} + \frac{1}{q_e} t \quad (14)$$

where K_2 = pseudo 2nd order rate constant (g mg⁻¹ min⁻¹).

The values of K_2 and R^2 show the continuous increasing trend for linear pseudo 2nd order, which confirms the suitability of this model for the adsorption of BF dye on the JSPB, but the nonlinear pseudo 2nd order does not fit with this process as R^2 has lower value comparatively.

Thermodynamic study. This study was conducted by shaking the 50 mL of the synthetic BF dye solution in the concentration range 25–100 mg L⁻¹ for different temperatures (308–328 K) at the optimum process conditions of pH 8.01,

contact time 75 min, dosage 0.6 g and concentration 100 mg L⁻¹ in the orbital shaker. At the end of shaking (after reaching equilibrium time), the flasks were withdrawn, solutions were filtered and the filtrates were analysed for the content of dye in the final solution using UV spectrophotometer. To know about the nature of the process, the thermodynamic parameters like Gibbs energy (ΔG^0), enthalpy (ΔH^0) and entropy (ΔS^0) changes were evaluated (Table IV).

The values of ΔH^0 and ΔS^0 were estimated from the plot of $\ln K_c$ vs. $1/T$. The negative value of ΔH^0 signify the exothermic nature of the process. The negative values of ΔG^0 show that the dye adsorption was spontaneous. The positive value of ΔS^0 points toward the increase in randomness due to interaction between adsorbent and dye molecules.

TABLE IV. Thermodynamic parameter for BF dye adsorption

Concentration mg L ⁻¹	ΔH^0 kJ mol ⁻¹	ΔS^0 J k ⁻¹ mol ⁻¹	ΔG^0 / kJ mol ⁻¹		
			308 K	318 K	328 K
25	-19.86	06.74	-0.093	-0.142	-0.228
50	-45.51	20.34	-1.709	-2.018	-2.112
75	-04.14	10.19	-2.721	-2.822	-2.924
100	-26.73	19.11	-3.215	-3.402	-3.597

Comparison study

The comparison study of obtained result with the reported results in literature are given in Table V. JSPB shows higher adsorption capacity compared to the reported data (Gupta *et al.*,¹⁰ Quin *et al.*,¹³ Kaith *et al.*,³⁷ Nwodika *et al.*¹⁵), while other adsorbents show higher adsorption capacity (Guan *et al.*;³⁸ Wang *et al.*³⁹) as they have used expensive chemicals to fabricate the adsorbent materials.

TABLE V. Comparison of adsorption capacity for BF dye removal with other literature data

Adsorbent	Adsorption capacity, mg g ⁻¹	Reference
Polymeric nanocomposite	0.439	Kaith <i>et al.</i> ³⁷
Graphite oxide	1.830	Quin <i>et al.</i> ¹³
Base activated cola nut pod carbon (KPBC)	3.470	Nwodika <i>et al.</i> ¹⁵
Acid activated cola nut pod carbon (KPBA)	5.760	Nwodika <i>et al.</i> ¹⁵
Bottom ash	6.400	Gupta <i>et al.</i> ¹⁰
Jamun seed powder biochar	8.000	Present study
Mesoporous molecular sieve of AI-SBA-16	70.080	Guan <i>et al.</i> ³⁸
Graphene based magnetic nanocomposite	89.400	Wang <i>et al.</i> ³⁹

CONCLUSION

The current study confirms that the JSPB is an effective, efficient and a low-cost adsorbent for the BF dye removal from synthetic waste water solution. The characterization shows that JSPB has good adsorption properties as it contains aromatic compounds and different elements like C, Mg, K, Si and Fe. The FT-IR

study reveals that biochar is rich in functional groups. The semi-crystalline surface of the biochar was revealed by the XRD analysis, which favours adsorption. The maximum removal efficiency and adsorption capacity of JSPB for BF dye removal was found to be 97 % and 8.0 g respectively at the optimum conditions of pH 8.01, concentration 100 mg L⁻¹, JSPB dosage 0.6 g, contact time 75 min and temperature 318 K. The adsorption capacity of JSPB is higher than other adsorbents (Table V) despite its fabrication through comparatively simple processes. The suitability of Temkin isotherm for both linear and non-linear forms indicate the uniform distribution of binding energy over the JSPB surface and also reveals that the adsorption heat for all molecules decreases with the increasing surface area of JSPB. Chemisorption behaviour of this process was confirmed by the linear pseudo-2nd order kinetic model. The negative values of ΔH^0 show the exothermic nature and the positive value of ΔS^0 indicates increase in randomness of the process. The overall study suggested that JSPB can be considered as eco-friendly and good adsorbent for the removal of cationic dyes.

ИЗВОД

УПОТРЕБА БИОУГЉА ОД СЕМЕНА *Syzyum cumini* ЗА УКЛАЊАЊЕ ФУКСИНСКЕ БОЈЕ ИЗ ВОДЕНОГ РАСТВОРА

DIVYA KOSALE, CHANDRAKANT THAKUR и VINOD KUMAR SINGH

Department of Chemical Engineering, National Institute of Technology Raipur, Raipur 492010, Chhattisgarh, India

Индустрија текстила, коже, боја и друге индустрије испуштају много боја у отпадне воде које могу имати велики утицај на животну средину и људски живот. Због тога је неопходно уклонити боју из отпадних вода пре њиховог испуштања и поновне употребе. У прошлости је предложено неколико поступака за уклањање и инактивацију боја, али је адсорпција стакла популарност због своје ефикасности и једноставне употребе. Употреба биоугљева као адсорбента добија на пажњи због њихове ниске цене, доступности и високе способности адсорпције. Ова студија је фокусирана на уклањање базног фуксина (BF) путем адсорпције ове боје, коришћењем биоугља у праху од семена *Syzyum cumini* као адсорбента. Биоугаљ је окарактерисан различитим анализама као што су: XRD, EDS, FTIR, TGA и SEM. Адсорпција је проучавана уз варирање параметара као што су рН, трајање контакта, температура, доза адсорбента и температура. Изотермна, кинетичка и термодинамичка испитивања су такође спроведена да би се разумео механизам адсорпције. Максимални капацитет адсорпције за BF боју је показао биоугаљ семена произведен на 500 °C. Ово истраживање открива да биоугаљ произведен од семена *Syzyum cumini* има значајан потенцијал за елиминацију BF боје из отпадних вода.

(Примљено 30. августа 2022, ревидирано 25. октобра 2022, прихваћено 9. априла 2023)

REFERENCES

1. B. Lellis, C. Z. Fávares-Polonio, J. A. Pamphile, J. C. Polonio, *Biotechnol. Res. Innov.* **3** (2019) 275 (<https://doi.org/10.1016/j.biori.2019.09.001>)
2. G. Mezohegyi, F. P. van der Zee, J. Font, A. Fortuny, A. Fabregat, *J. Environ. Manage.* **102** (2012) 148 (<https://doi.org/10.1016/j.jenvman.2012.02.021>)

3. S. Punathil, D. Ghime, T. Mohapatra, C. Thakur, P. Ghosh, *J. Hazard. Toxic Radioact. Waste* **24** (2020) 2 ([https://doi.org/10.1061/\(asce\)hz.2153-5515.0000534](https://doi.org/10.1061/(asce)hz.2153-5515.0000534))
4. V. Chandane, V. K. Singh, *Desalin. Water Treat.* **57** (2016) 4122 (<https://doi.org/10.1080/19443994.2014.991758>)
5. V. Kumar, A. Khapre, C. Thakur, P. Ghosh, P. K. Chaudhari, *Int. J. Chem. React. Eng.* (2021) (<https://doi.org/10.1515/ijcre-2021-0175>)
6. S. Barakan, V. Aghazadeh, *Environ. Sci. Pollut. Res.* **28** (2021) 2572 (<https://doi.org/10.1007/s11356-020-10985-9>)
7. P. K. Navin, S. Kumar, M. Mathur, *Int. J. Eng. Res. Technol.* **6** (2018) 1 (<https://www.ijert.org/research/textile-wastewater-treatment-a-critical-review-IJERTCONV6IS11015.pdf>)
8. M. Paredes-Laverde, M. Salamanca, J. D. Diaz-Corrales, E. Flórez, J. Silva-Agredo, R. A. Torres-Palma, *J. Environ. Chem. Eng.* **9** (2021) (<https://doi.org/10.1016/j.jece.2021.105685>)
9. K. Sarayu, S. Sandhya, *Appl. Biochem. Biotechnol.* **167** (2012) 645 (<https://doi.org/10.1007/s12010-012-9716-6>)
10. V. K. Gupta, A. Mittal, V. Gajbe, J. Mittal, *J. Colloid Interface Sci.* **319** (2008) 30 (<https://doi.org/10.1016/j.jcis.2007.09.091>)
11. M. El-Azazy, A. S. El-Shafie, A. Ashraf, A. A. Issa, *Appl. Sci.* **9** (2019) (<https://doi.org/10.3390/app9224855>)
12. M. El Haddad, *J. Taibah Univ. Sci.* **10** (2016) 664 (<https://doi.org/10.1016/j.jtusci.2015.08.007>)
13. J. Qin, F. Qiu, X. Rong, J. Yan, H. Zhao, D. Yang, *Toxicol. Environ. Chem.* **96** (2014) 849 (<https://doi.org/10.1080/02772248.2014.993642>)
14. Priya, B. S. Kaith, U. Shanker, B. Gupta, *J. Environ. Manage.* **234** (2019) 345 (<https://doi.org/10.1016/j.jenvman.2018.12.117>)
15. N. Chekwube, O. D. Onukwuli, *Gazi Univ. J. Sci.* **30** (2017) 86
16. X. Zhang, J. Huang, Z. Kang, D. P. Yang, R. Luque, *Mol. Catal.* **484** (2020) 110786 (<https://doi.org/10.1016/j.mcat.2020.110786>)
17. S. Kalita, M. Pathak, G. Devi, H. P. Sarma, K. G. Bhattacharyya, A. Sarma, A. Devi, *RSC Adv.* **7** (2017) 27248 (<https://doi.org/10.1039/c7ra03014b>)
18. A. Sagar, A. Dubey, *Int. J. Chem. Studies* **7** (2019) 590 (<https://www.chemjournal.com/archives/2019/vol7issue3/PartK/7-2-227-854.pdf>)
19. M. El Haddad, *Integr. Med. Res.* **10** (2018) 664 (<https://doi.org/10.1016/j.jtusci.2015.08.007>)
20. J. N. Nsami, J. K. Mbadcam, *J. Chem.* **2013** (2013) 469170 (<https://doi.org/10.1155/2013/469170>)
21. K. I. Aly, M. M. Sayed, M. G. Mohamed, S. W. Kuo, O. Younis, *Micropor. Mesopor. Mater.* **298** (2020) 110063 (<https://doi.org/10.1016/j.micromeso.2020.110063>)
22. M. Stylianou, A. Christou, P. Dalias, P. Polycarpou, C. Michael, A. Agapiou, P. Papanastasiou, D. Fatta-Kassinos, *J. Energy Inst.* **93** (2020) 2063 (<https://doi.org/10.1016/j.joei.2020.05.002>)
23. D. Özçimen, A. Ersoy-Meriçboyu, *Renew. Energy* **35** (2010) 1319 (<https://doi.org/10.1016/j.renene.2009.11.042>)
24. D. Zhang, T. Wang, J. Zhi, Q. Zheng, Q. Chen, C. Zhang, Y. Li, *Materials (Basel)* **13** (2020) 1 (<https://doi.org/10.3390/ma13245594>)

25. E. O. Oyelude, F. Frimpong, D. Dawson, *J. Mater. Environ. Sci.* **6** (2015) 1126
(https://www.jmaterenvironsci.com/Document/vol6/vol6_N4/132-JMES-1383-2015-Oyelude.pdf)
26. V. K. Singh, A. B. Soni, R. K. Singh, *Orient. J. Chem.* **32** (2016) 2621
(<https://doi.org/10.13005/ojc/320534>)
27. W. Bessashia, Y. Berredjem, Z. Hattab, M. Bououdina, *Environ. Res.* **186** (2020) 109484
(<https://doi.org/10.1016/j.envres.2020.109484>)
28. F. Mashkoo, A. Nasar, Inamuddin, A. M. Asiri, *Sci. Rep.* **8** (2018) 1
(<https://doi.org/10.1038/s41598-018-26655-3>)
29. T. A. Khan, E. A. Khan, Shahjahan, *Appl. Clay Sci.* **107** (2015) 70
(<https://doi.org/10.1016/j.clay.2015.01.005>)
30. R. Bhattacharyya, S. K. Ray, *Polym. Eng. Sci.* **53** (2013) 2439
(<https://doi.org/10.1002/pen.23501>)
31. N. Abdus-Salam, A. V. Ikudayisi-Ugbe, F. A. Ugbe, *Chem. Data Collect.* **31** (2021) 100626
(<https://doi.org/10.1016/j.cdc.2020.100626>)
32. L. Wang, J. Zhang, A. Wang, *Colloids Surfaces, A* **322** (2008) 47
(<https://doi.org/10.1016/j.colsurfa.2008.02.019>)
33. S. Parimal, M. Prasad, U. Bhaskar, *Ind. Eng. Chem. Res.* **49** (2010) 2882
(<https://doi.org/10.1021/ie9013343>)
34. K. Patidar, M. Vashishtha, *J. Serbian Chem. Soc.* **86** (2021) 429
(<https://doi.org/10.2298/JSC201103010P>)
35. A. A. Babaei, S. N. Alavi, M. Akbarifar, K. Ahmadi, A. Ramazanpour Esfahani, B. Kakavandi, *Desalin. Water Treat.* **57** (2016) 27199
(<https://doi.org/10.1080/19443994.2016.1163736>)
36. D. Tian, X. Zhang, C. Lu, G. Yuan, W. Zhang, Z. Zhou, *Cellulose* **21** (2014) 473
(<https://doi.org/10.1007/s10570-013-0112-3>)
37. B. Singh, U. Shanker, B. Gupta, *J. Environ. Manage.* **234** (2019) 345
(<https://doi.org/10.1016/j.jenvman.2018.12.117>)
38. Y. Guan, S. Wang, C. Sun, G. Yi, X. Wu, L. Chen, X. Ma, *Chem. Pap.* **73** (2019) 2655
(<https://doi.org/10.1007/s11696-019-00817-7>)
39. C. Wang, C. Feng, Y. Gao, X. Ma, Q. Wu, Z. Wang, *Chem. Eng. J.* **173** (2011) 92
(<https://doi.org/10.1016/j.cej.2011.07.041>).